Design of CT and CQ Filters Using Approximation and Optimization

Ralph Levy, *Life Fellow, IEEE,* and Peter Petre, *Member, IEEE*

***Abstract*—A new design technique for cascaded triplet (CT) filters has been derived commencing from the well-known Chebyshev all-pole prototype filter. One or more finite frequency poles may be introduced by cross coupling across sets of three nodes, and the filter rematched by a reasonably accurate approximate compensation of the element values. Any general optimizer may then be used to obtain a nearly perfect result without undue concern over convergence failures. A previous similar theory for cascaded quadruplet sections is generalized and may be combined with the CT theory to form filters having both types of sections. The theory is applied to both singly and doubly terminated filters and may include poles on the real axis of the s-plane for delay equalization.**

***Index Terms*—Cascaded trisection filters, cascaded quadruplet filters, cross-coupled filters, filter synthesis and optimization, singly and doubly terminated filters.**

I. Introduction

THIS PAPER focuses on the design of filters having cascaded triplet (CT) or cascaded quadruplet (CQ) sections that are relatively simple to tune compared with filters having "nested" cross couplings. The latter may have more optimal characteristics but are typically much more difficult to align and tune. Exact design theories using classical synthesis are available [1]–[3], but recently there has been interest in design techniques based on optimization [4], [5]. If optimization is to be used, it is preferable to commence from a design that is as close as possible to the final result (i.e., an approximate theory is desirable). This design is available for filters having CQ sections [6] but not for CT sections. It is perhaps surprising that the exact design theory for CT sections has preceded the approximate one given in this paper.

The selection of filter degree with transmission zero locations has been the subject of many previous papers, e.g., [1]–[5]. As a general rule, a simple Chebyshev filter would be designed initially, and, if it fails to meet specifications, one or more poles are shifted from dc and/or infinity to improve the response. Also, in most cases, the overall degree will be reduced compared with the initial Chebyshev design since a pseudo-elliptic filter with poles of attenuation is much more efficient. Frequently specifications may be met by more than one set of design parameters. The attenuation poles in the final prototype design are realized using cross coupling in the form of CT and/or CQ sections as described in this work and in previous papers.

Manuscript received March 30, 2001; revised September 1, 2001.

R. Levy is with R. Levy Associates, La Jolla, CA 92037 USA (e-mail: r.levy@ieee.org).

P. Petre is with the Microelectronics Laboratory, HRL Laboratories, LLC, Malibu, CA 90265 USA (e-mail: petre@hrl.com).

Publisher Item Identifier S 0018-9480(01)10458-8.

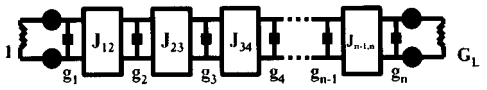

Fig. 1. Doubly terminated low-pass prototype filter.

Although in many cases it is possible to optimize a design starting from the correct topology but with arbitrarily assigned element values, such methods may not always converge, especially for high-degree filters. Thus, the objective function given in [4] does not apply to CQ sections producing real axis transmission zeros used in linear-phase filters. Usually it is preferable to commence from a close approximate design that is almost certainly guaranteed to converge using any standard optimizer. In addition, the existence of an approximate design may be considered to be of academic interest and to have practical engineering value. The question of why optimization should be used when exact synthesis theory exists is also pertinent, but synthesis may not always be simple or readily available, and many engineers would prefer more commonly used procedures. The present combination of a relatively good approximation followed by rapid optimization is simpler and may be considered more general as far as ease of application is concerned, compared with exact synthesis for complex situations (e.g., multiplexers where the input match almost always requires additional optimization beyond the result obtained from exact synthesis).

II. Theory of Cascaded CT Sections

The theory commences from the standard all-pole low-pass prototype filter shown in Fig. 1, which will normally have a Chebyshev equi-ripple response, but could also be Butterworth or correspond to other specialized responses. This filter is converted into a bandpass filter with band edges ω_1 and ω_2, and normalized mid-band frequency

$$\omega_0 = \sqrt{\omega_1 \omega_2}. \tag{1}$$

The admittance inverters may be realized as standard Pi sections of capacitors or inductors [7], as shown in Fig. 2(a) for capacitive (pole at dc) and Fig. 2(b) for inductive (pole at infinity) inverters, but there is a third realization shown in Fig. 2(c), which is to use a Pi of parallel *LC* sections [8], [9]. This introduces a pole at

$$\omega_p = 1/\sqrt{LC} \tag{2}$$

and is the basis of the theory.

It is well known that in standard C- or L-type Pi sections the negative shunt circuit elements are absorbed into the adjacent

0018–9480/01$10.00 © 2001 IEEE

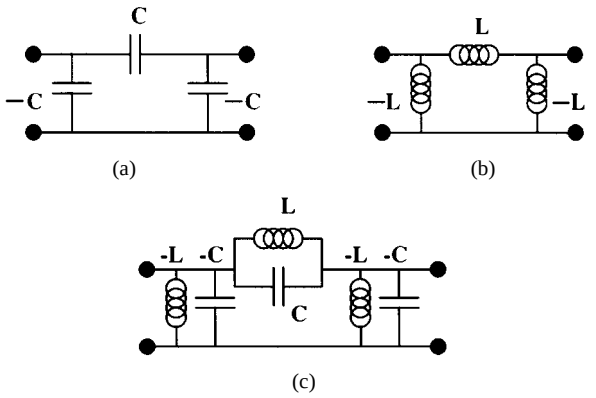

Fig. 2. (a) Capacitive ($J = \omega_0 C$). (b) Inductive ($J = 1/\omega_0 L$). (c) Pole-producing admittance inverters ($J = \omega_0 C - 1/\omega_0 L$.)

main positive shunt elements. The same absorption procedure is used for the finite frequency pole-producing sections.

The LC product is given by the resonant condition (2), and the value of C and L is determined by the required value of the admittance inverter J at mid-band. Assuming admittances normalized to 1 Ω, the susceptance of the inverter of Fig. 2(c) is

$$\omega_0 C - 1/\omega_0 L = J \tag{3}$$

where ω_o is the mid-band or synchronous frequency of the filter. The values of C and L are then obtained from (2) and (3). Note that J is positive if the pole lies above the passband and negative if below. In either case, we obtain the result

$$\omega_0 C = J/\left(\omega_p^2 - \omega_0^2\right) \tag{4}$$

and

$$L = 1/\left(\omega_p^2 C\right) \tag{5}$$

giving positive values of C and L.

The case where the pole is on the real axis at $s = \sigma$, giving delay equalization, is also of interest. Here, the values of C and L may be derived by carrying out the substitution

$$\omega_p = -j\sigma \tag{6}$$

in (4) and (5), leading to

$$\omega_0 C = -J/\left(\sigma^2 + \omega_0^2\right) \tag{7}$$

and

$$L = -1/\left(\sigma^2 C\right). \tag{8}$$

J is positive for such sections, so that C is negative and L positive, a result which has been described previously (e.g., in [2, Fig. 8]). This particular type of real axis pole may be produced only by a CQ, not by a CT section.

Following formation of all of the admittance inverters, the resulting LC circuits with real frequency poles may then be converted into ones having CT sections using the formulas given in [3]. Since apparently this reference is not readily available to many readers, the formulas are reproduced in the Appendix for completeness. The overall procedure guarantees that the pole is produced at the correct frequency, and that the return loss is correct at mid-band.

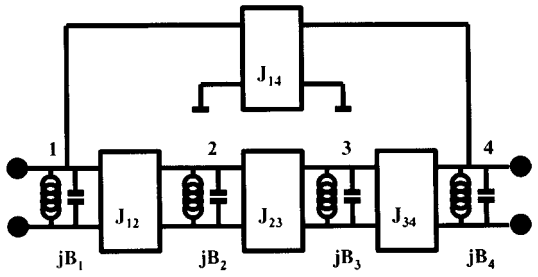

Fig. 3. Formation of a bandpass CQ section.

III. Theory of General CQ Sections

The original theory given in [6] is presented for symmetrical sections of a low-pass prototype filter. Here, we require formation of cross-coupled asymmetric bandpass CQ sections.

Commencing from a four-node portion of a bandpass filter derived from a standard low-pass prototype as shown in Fig. 3, we need to introduce a cross coupling across nodes 1 and 4 to introduce poles at real frequencies or on the real axis of the complex frequency plane s. The admittance to ground at node i is

$$jB_i = jg_i \frac{(\omega/\omega_0 - \omega_0/\omega)}{w} \tag{9}$$

where the fractional bandwidth is

$$w = \frac{(\omega_2 - \omega_1)}{\omega_0}. \tag{10}$$

The admittance matrix of the network, neglecting the shunt susceptances at nodes 1 and 4, which do not enter into the final equations, is

$$j\begin{bmatrix} 0 & -J_{12} & 0 & -J_{14} \\ -J_{12} & B_2 & -J'_{23} & 0 \\ 0 & -J'_{23} & B_3 & -J_{34} \\ -J_{14} & 0 & -J_{34} & 0 \end{bmatrix} \tag{11}$$

where J'_{23}, the value obtained from the prototype Chebyshev low-pass filter, has been amended to J'_{23}, since its value will be changed in the cross-coupled section. The matrix of (11) gives the following set of equations:

$$\begin{aligned} I_1 &= -jJ_{12}V_2 - jJ_{14}V_4 \\ I_2 &= -jJ_{12}V_1 + jB_2V_2 - jJ'_{23}V_3 \\ I_3 &= -jJ'_{23}V_2 + jB_3V_3 - jJ_{34}V_4 \\ I_4 &= -jJ_{14}V_1 - jJ_{34}V_3. \end{aligned} \tag{12}$$

The next step is to form the 2×2 matrix of the section between nodes 1 and 4 (i.e., that relating currents I_1 and I_4 to voltages V_1 and V_4 with $I_2 = I_3 = 0$ since there are no impressed current sources at nodes 2 and 3).

The second and third equations in (12) become

$$\begin{aligned} B_2V_2 - J'_{23}V_3 &= J_{12}V_1 \\ -J'_{23}V_2 + B_3V_3 &= J_{34}V_4. \end{aligned} \tag{13}$$

Writing (13) in matrix form and inverting gives

$$\begin{bmatrix} V_2 \\ V_3 \end{bmatrix} = \frac{j}{\Delta} \begin{bmatrix} B_3 & -J'_{23} \\ -J'_{23} & B_2 \end{bmatrix} \begin{bmatrix} I_2 \\ I_3 \end{bmatrix} \tag{14}$$

where

$$\Delta = B_2 B_3 - J'^2_{23}. \tag{15}$$

We can now substitute for V_2 and V_3 in the first and fourth equations of (12) to give the required two-port admittance matrix as

$$\begin{bmatrix} y_{11} & y_{14} \\ y_{41} & y_{44} \end{bmatrix} \tag{16}$$

where

$$\begin{aligned} y_{11} &= -jB_3\, J_{12}^2/\Delta \\ y_{14} &= -j\,(J_{14} + J_{12}\, J'_{23} J_{34}/\Delta) = y_{41} \\ y_{44} &= -jB_2\, J_{34}^2/\Delta. \end{aligned} \tag{17}$$

The condition for the occurrence of attenuation poles is there shall be no transmission between nodes 1 and 4 (i.e., $y_{14} = 0$), which, from (17) and (15), gives

$$J_{14} = -\frac{J_{12} J'_{23} J_{34}}{B_2 B_3 - J'^2_{23}}. \tag{18}$$

This is seen to be a generalization of [6, eq. (15)], where we recover the latter if we have $J_{12} = J_{34} = 1$, $J'_{23} = J'_m$, and $G_2 = G_3 = ag_m$. Using (9), we see that attenuation poles occur when

$$J_{14} = \frac{-J_{12} J'_{23} J_{34}}{g_2 g_3 \left[(\omega_p/\omega_0 - \omega_0/\omega_p)/w\right]^2 - J'^2_{23}}. \tag{19}$$

Equation (19) gives poles denoted by ω_{p1} and ω_{p2} on each side of the passband, where

$$\omega_{p1}\omega_{p2} = \omega_0^2. \tag{20}$$

Thus we may select one of these poles, and the other is forced to occur in accordance with (20).

In order to complete the necessary set of equations, the condition for a match at mid-band is obtained similarly to that described in [6] (i.e., by forming the admittance matrix 1–4 with $J_{14} = 0$ and equating the perturbed and unperturbed y_{14} terms at mid-band). Thus, using (15) with $B_2 = B_3 = 0$, giving $\Delta = -J'^2_{23}$, we find from (17)

$$J_{14} - J_{12} J_{34}/J'_{23} = -J_{12} J_{34}/J_{23}$$

or

$$J'_{23} = \frac{J_{12} J_{23} J_{34}}{J_{12} J_{34} + J_{14} J_{23}}. \tag{21}$$

This is seen to be identical to [6, eq. (17)] if $J_{12} = J_{34} = 1$, $J_{23} = J_m$, $J'_{23} = J'_m$, and $J_{14} = J_{m-1}$.

Hence, given a pole frequency ω_{p1}, which determines ω_{p2} from (20), we may solve for the unknowns J_{14} and J'_{23} from (19) and (21).

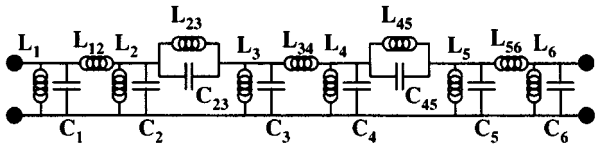

Fig. 4. N = 6 filter with two coincident poles. These may be converted into CT sections using matrix operations which removes capacitor 2–3 and introduces one across 1–3, with a similar operation to remove 4–5 and introduce 4–6.

In the case of real axis zeros located at $s = \pm\sigma$, (19) becomes

$$J_{14} = \frac{J_{12} J'_{23} J_{34}}{g_2 g_3 \left[(\sigma/\omega_0 + \omega_0/\sigma)/w\right]^2 + J'^2_{23}}. \tag{22}$$

The theory will now be illustrated by several examples.

IV. Examples

A. Example 1—Doubly Terminated CT Filters

Here, we illustrate the design of six-section filters having two coincident poles. The lumped-element circuit is shown in Fig. 4 and was derived from the prototype of Fig. 1 using three inductive and two pole-producing pi inverters. This topology is appropriate for eventual conversion into a combline filter using Richards' transformation and well-known close approximation techniques. The ripple level is 20-dB return loss, and the return-loss bandwidth is 5%. Frequencies are normalized to mid-band with band edges at 0.975 and 1.025. The two examples are for poles located at 0.90 and 0.95, respectively, and the comparisons between the exact and approximate theories are given in Table I(a) and (b). The maximum errors for the element values are approximately 2% for the pole at 0.90 and 7.7% for that at 0.95. Such relatively small error is the reason for the suitability of the method for optimization.

Analysis of the case with the pole at 0.9 showed a return loss of better than 11 dB, and the bandwidth shifted slightly higher in frequency. The analysis for the more severe case with the pole at 0.95, which is much closer to the passband edge, is shown in Fig. 5. Here, the return loss has degraded to a worst level of 6.5 dB and the frequency shift has increased. However, the return-loss poles appear to be present and the form of the characteristics suitable for optimization. In practice, in both cases, the filters optimized within a few seconds using a standard gradient-based optimizer, here "Touchstone." Since the approximation is so close to the exact result, the details of the optimization are unimportant, and almost any optimization technique should be successful. In our case, 100 frequencies were used, spread across the passbands and stopbands, and simple constraints on the passband return loss and stopband rejection were applied.

The optimized result for the pole at 0.95 is shown in Fig. 6. The six return-loss poles are well resolved, and the 20-dB return-loss level is produced quite closely. The result was obtained by retaining the element values of the pole-producing sections, which appears to be possible in all cases so far investigated. This fact, combined with the nonunique nature of the bandpass filter (it has an infinite number of equivalent circuits), means that the final set of element values differ slightly from those of the exact synthesis.

TABLE I
COMPARISON BETWEEN EXACT AND APPROXIMATE ELEMENT VALUES FOR SIX-SECTION FILTERS HAVING POLE PAIRS AT COINCIDENT FREQUENCIES. (a) POLES AT 0.90. (b) POLES AT 0.95. (SEE FIG. 3 FOR CIRCUIT TOPOLOGY)

	Exact		Approximate	
	Capacitance	Inductance	Capacitance	Inductance
C_1, L_1	19.9182	0.0523	19.9096	0.0525
L_{12}	-	1.2039	-	1.1912
C_2, L_2	16.753	0.0611	16.7069	0.0607
C_{23}, L_{23}	3.2628	0.3784	3.2027	0.3855
C_3, L_3	16.7431	0.0600	16.7069	0.0598
L_{34}	-	1.7595	-	1.7213
C_4, L_4	16.7431	0.0600	16.7069	0.0598
C_{45}, L_{45}	3.2628	0.3784	3.2027	0.3855
C_5, L_5	16.753	0.0611	16.7069	0.0607
L_{56}	-	1.2039	-	1.1912
C_6, L_6	19.9182	0.0523	19.9096	0.0525

(a)

	Exact		Approximate	
	Capacitance	Inductance	Capacitance	Inductance
C_1, L_1	19.9201	0.0522	19.9096	0.0525
L_{12}	-	1.2561	-	1.1913
C_2, L_2	13.4006	0.0775	13.6684	0.0745
C_{23}, L_{23}	6.7210	0.1649	6.2411	0.1775
C_3, L_3	13.3768	0.0757	13.6684	0.0731
L_{34}	-	1.9175	-	1.7213
C_4, L_4	13.3768	0.0757	13.6684	0.0731
C_{45}, L_{45}	6.7210	0.1649	6.2411	0.1775
C_5, L_5	13.4006	0.0775	13.6684	0.0745
L_{56}	-	1.2561	-	1.1913
C_6, L_6	19.9201	0.0522	19.9096	0.0525

(b)

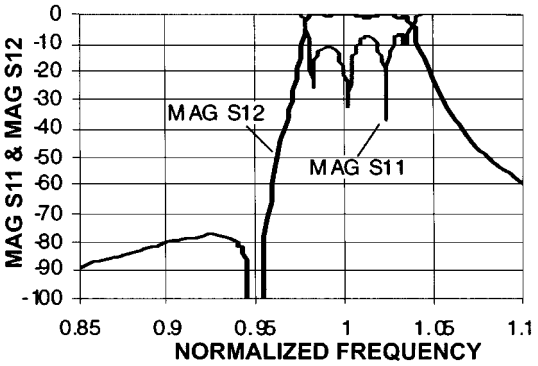

Fig. 5. Results for the approximate design.

B. Example 2—Singly Terminated CT-Filters

1) Low-Pass Prototype Element Values: Singly terminated filters are used in the design of contiguous multiplexers, and an example is included here to illustrate this general case, which requires a different type of optimization condition than normal matched doubly terminated filters. A second objective is to present suitable formulas for the Chebyshev low-pass prototype, which are not always correct in the available literature.

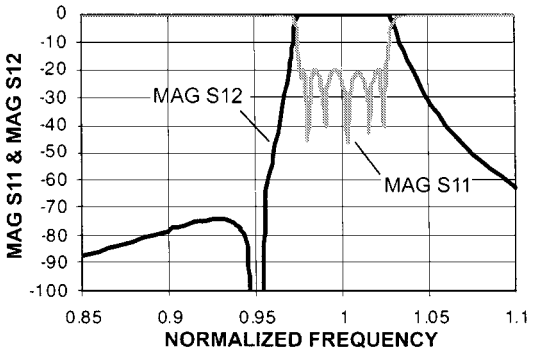

Fig. 6. Design of Fig. 4 after optimization.

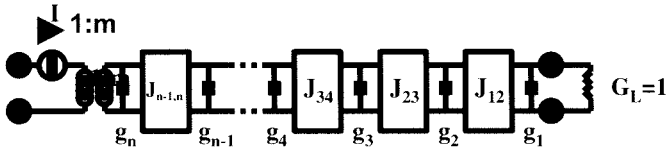

Fig. 7. Singly terminated low-pass prototype filter.

The circuit of the prototype with admittance inverters, all-shunt elements, and unity terminating conductance for both even and odd values of filter degree n is given in Fig. 7. The insertion loss function for the Chebyshev case is

$$A = 1 + h^2 T_n^2(\omega') \tag{23}$$

and almost correct formulas and tables for the g values are given in [10, pp. 107–109]. The formulas are correct for n odd and for n even, apart from an ideal transformer missing from the infinite-impedance end for n even. The g values are given by

$$g_1 = \frac{\sin(\pi/2n)}{\gamma} \tag{24}$$

$$g_r g_{r+1} = \frac{\sin\left[(2r-1)\pi/2n\right]\sin\left[(2r+1)\pi/2n\right]}{\cos^2\left[r\pi/2n(\gamma^2+\sin^2(r\pi/2n))\right]} \tag{25}$$

$$J_{r,r+1} = 1 \qquad (r = 1, 2, \ldots, n-1) \tag{26}$$

and

$$G_L = 1 \tag{27}$$

where

$$\gamma = \sinh\left[(1/n)\sinh^{-1}(1/h)\right]. \tag{28}$$

In the case of n even, we define

$$m = \frac{(S+1)}{2\sqrt{S}} \tag{29}$$

where S is the ripple level expressed as a voltage standing-wave ratio (VSWR), i.e.,

$$S = \left[h + \sqrt{1+h^2}\right]^2. \tag{30}$$

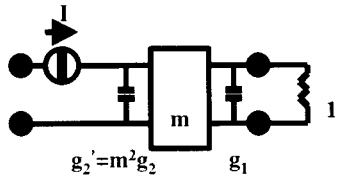

(a)

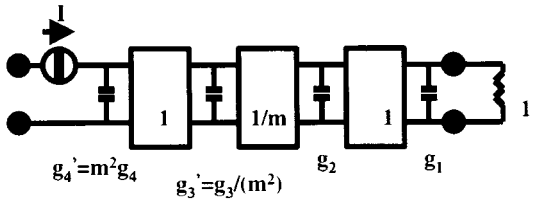

(b)

Fig. 8. Modified singly terminated low-pass prototypes of even order: (a) $n = 2$ and (b) $n = 4$.

TABLE II
SINGLY TERMINATED LOW-PASS PROTOTYPE FILTERS, 0.5-dB RIPPLE, $M = 1.059254$. SEE FIG. 8 FOR TOPOLOGY

N=2		N=4		N=6		N=8	
g_1	0.701447	g_1	0.835515	g_1	0.862682	g_1	0.872539
J_{12}	1.059254	g_2	1.391574	g_2	1.448274	g_2	1.466564
g_2	1.054989	J_{23}	0.944061	g_3	1.849375	g_3	1.878567
		g_3	1.539988	J_{34}	1.059254	g_4	1.750772
		g_4	1.474053	g_4	1.918815	J_{45}	0.944061
				g_5	1.695006	g_5	1.780704
				g_6	1.575550	g_6	2.002413
						g_7	1.744292
						g_8	1.613365

It is convenient to replace the ideal transformer by a central admittance inverter of value given by

$$J_{n/2,\,n/2+1} = m \quad (n \text{ even}, n/2 \text{ odd}) \tag{31a}$$

$$J_{n/2,\,n/2+1} = 1/m \quad (n \text{ even}, n/2 \text{ even}). \tag{31b}$$

In this case, it is necessary to modify the g values g_r for $r = n, n-1, \ldots, n/2$, as indicated in Fig. 8, showing modified values for $n = 2$ and $n = 4$. Tabulated values for 0.5-dB ripple prototypes for n even are shown in Table II.

2) Singly Terminated CT Filter, $n = 5$: The example is a five-section singly terminated filter designed for normalized passband edges of 0.975 to 1.025, and a pair of coincident poles at 0.850. The ripple level is 0.512 dB, and, using (23)-(28), the g values are 0.858624, 1.430563, 1.818968, 1.641949, and 1.541968 (infinite impedance end). Equations (4) and (5) are used to introduce the poles at 0.850, resulting in the circuit of Fig. 9. When used in multiplexers, such filters are connected at the infinite impedance end, and it is logical then to reverse the nodal nomenclature, as in Table III, which shows a comparison between the exact and approximate values of the circuit elements. The normalized real part of the input impedance of a singly terminated filter of this type should be equi-ripple and less than unity, in the present case varying between 0.8889, and 1. Fig. 10 shows the real and imaginary parts of this impedance for the approximate theory. Optimization is then applied, with the objective function forcing the real part to lie between the assigned limits of 0.8889 and 1, and the result obtained is shown in Fig. 11. The optimization time is substantially instantaneous.

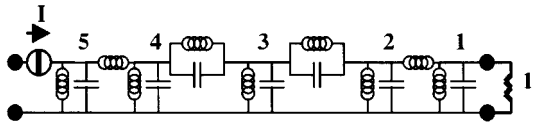

Fig. 9. $N = 5$ singly terminated filter prior to conversion into CT format.

TABLE III
COMPARISON BETWEEN EXACT AND APPROXIMATE ELEMENT VALUES FOR FILTER OF FIG. 9

NODES		Exact		Approximate	
		C	L	C	L
1	0	30.667958	0.033677	30.830078	0.033545
1	2	0	1	0	1
2	0	29.735002	0.033793	29.225112	0.034241
2	3	3.603604	0.384083	3.603599	0.384084
3	0	28.724072	0.032955	29.160800	0.032115
3	4	3.603604	0.384083	3.603599	0.384084
4	0	25.351571	0.039689	24.998720	0.040031
4	5	0	1	0	1
5	0	17.171453	0.061730	17.167105	0.061895

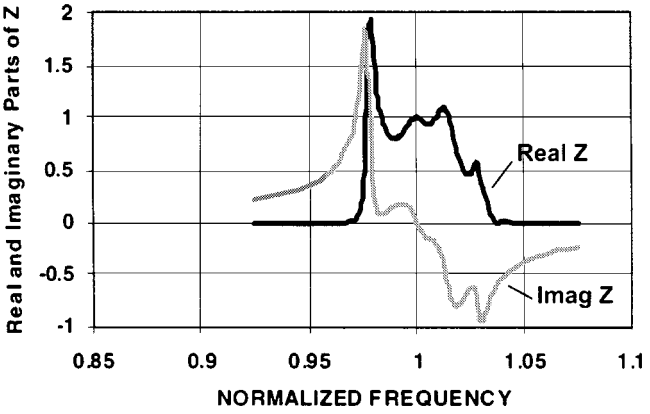

Fig. 10. Real and imaginary parts of Z_{in} for $N = 5$ singly terminated filter with poles at 0.85: approximate theory, before optimization.

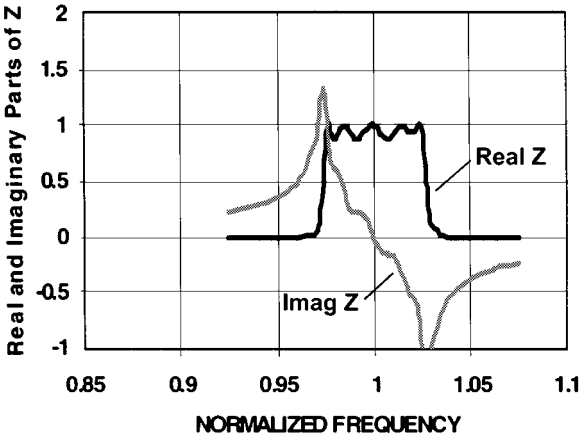

Fig. 11. Real and imaginary parts of Z_{in} for $N = 5$ singly terminated filter with poles at 0.85: after optimization.

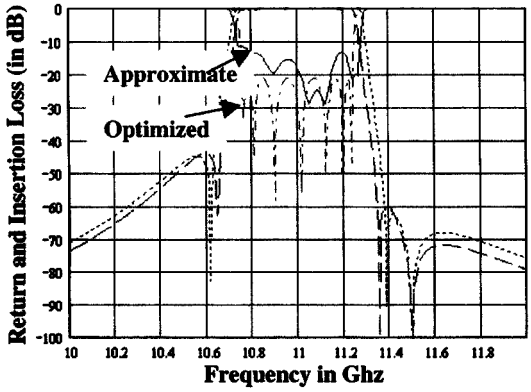

Fig. 12. Approximate and optimized results for an $n = 7$ CQ/CT filter.

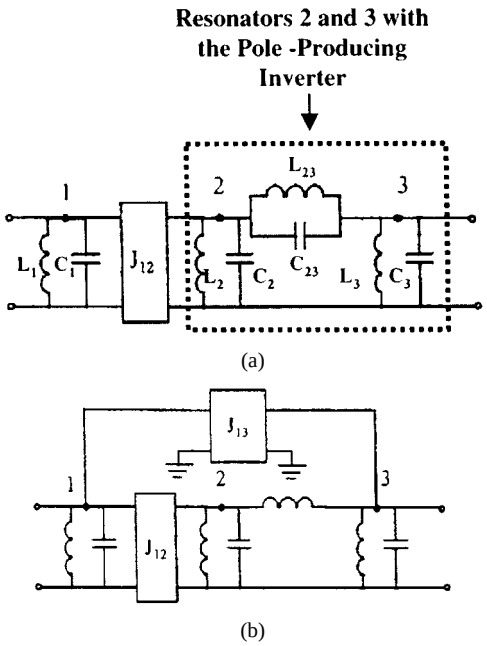

Fig. 13. (a) Pole-producing inverter introduced replacing in the bandpass prototype. (b) Series capacitator eliminated by introducing cross coupling between resonator 1 and 3.

C. Example 3—$N = 7$ CQ/CT Filter

The entire theory may be expressed in terms of the coupling matrix, the elements of which are related to the element values of the filter by the well-known relationship

$$M_{ij} = \frac{J_{ij}}{\sqrt{g_i g_j}}. \tag{32}$$

We propose to defer further details for a later paper. This particular method was applied to the design of an $n = 7$ filter consisting of a CQ section between nodes 1 and 4, producing a pair of finite frequency poles, and a CT section between nodes 5 and 7, giving an extra high side pole. In this example, the approximate theory gives remarkably good results, as seen in Fig. 12, which also gives the optimized result.

V. Conclusion

A new theory for the design of CT filters based on derivation of specific design equations and the element values of the standard Chebyshev all-pole low-pass filter has been described. If the finite attenuation poles are relatively far from the passband, then the theory may be quite accurate, but optimization is usually required, and convergence is practically guaranteed since the starting condition is sufficiently close to the final ideal result. The new results complement an earlier one obtained for CQ filters [6], and both CT and CQ sections may be incorporated within a filter design.

Appendix
Formulas for Conversion of a Cascaded Pole Section to a CT Section [3]

The admittance matrix of the circuit shown in Fig. 13(a) is

$$j\begin{bmatrix} B_1 & -J_{12} & 0 \\ -J_{12} & B_2+B_3 & -B_{23} \\ 0 & -B_{23} & B_3+B_{23} \end{bmatrix} \tag{33}$$

where

$$B_i = sC_i + \frac{1}{sL_i} \tag{34}$$

$$B_{ij} = sC_{ij} + \frac{1}{sL_{ij}} \tag{35}$$

and s is the complex frequency variable.

Row 2 and column 2 of (33) are multiplied by a factor m and added to row 3 and column 3, respectively, giving a new 3×3 admittance matrix

$$j\begin{bmatrix} B_1 & -J_{12} & -mJ_{12} \\ -J_{12} & B_2+B_{23} & m(B_2+B_{23})-B_{23} \\ -mJ_{12} & m(B_2+B_{23})-B_{23} & \begin{matrix} B_{23}+B_3-2mB_{23}+ \\ +m^2(B_{23}+B_3) \end{matrix} \end{bmatrix} \tag{36}$$

which has a two-port transfer function equivalent to that of the original circuit. A cross-coupling inverter mJ_{12} has been introduced in (36). The capacitor from the admittance in the matrix elements 2–3 and 3–2 is now eliminated to leave a simple series inductor as shown in Fig. 13(b), giving

$$m = \frac{C_{23}}{C_2 + C_{23}} \tag{37}$$

and the remaining inductance across nodes 2 and 3 is L_{23}, given by

$$\frac{1}{L'_{23}} = m\left(\frac{1}{L_2} + \frac{1}{L_{23}}\right) - \frac{1}{L_{23}}. \tag{38}$$

The remaining circuit elements of the CT section may be written down from matrix (36) in conjunction with (37).

References

[1] R. J. Cameron and J. D. Rhodes, "Asymmetric realizations for dual-mode bandpass filters," *IEEE Trans. Microwave Theory Tech.*, vol. MTT-29, pp. 51–58, Jan. 1981.

[2] R. Levy, "Direct synthesis of cascaded quadruplet (CQ) filters," *IEEE Trans. Microwave Theory Tech.*, vol. 43, pp. 2940–2945, Dec. 1995.

[3] R. Hershtig, R. Levy, and K. A. Zaki, "Synthesis and design of cascaded trisection (CT) dielectric resonator filters," in *Eur. Microwave Conf. Dig.*, Jerusalem, Israel, 1997, pp. 784–791.
[4] W. A. Atia, K. A. Zaki, and A. E. Atia, "Synthesis of general topology multiple coupled resonator filters by optimization," in *IEEE MTT-S Int. Microwave Symp. Dig.*, June 1998, pp. 821–824.
[5] S. Amari, "Synthesis of cross-coupled resonator filters using an analytical gradient-based optimization technique," *IEEE Trans. Microwave Theory Tech.*, vol. 48, pp. 1559–1564, Sept. 2000.
[6] R. Levy, "Filters with single transmission zeros at real and imaginary frequencies," *IEEE Trans. Microwave Theory Tech.*, vol. MTT-24, pp. 172–182, Apr. 1976.
[7] S. B. Cohn, "Direct-coupled resonator filters," *Proc. IRE*, vol. 45, pp. 187–196, Feb. 1957.
[8] R. Levy, "Mixed lumped and distributed linear-phase filters," in *Eur. Microwave Circuit Theory Design Conf.*, London, U.K., July 1974, Conf. Pub. 116, pp. 32–37.
[9] R. Levy and K. J. Andersen, "An optimal low loss HF diplexer using helical resonators," in *IEEE MTT-S Int. Microwave Symp. Dig.*, June 1992, pp. 1187–1190.
[10] G. L. Matthaei, L. Young, and E. M. T. Jones, *Microwave Filters, Impedance-Matching Networks, and Coupling Structures*. New York: McGraw-Hill, 1964.

Ralph Levy (SM'64–F'73–LF'99) received the B.A. and M.A. degrees in physics from Cambridge University, Cambridge, U.K., in 1953 and 1957, respectively, and the Ph.D. degree in applied sciences from London University, London, U.K., in 1966.

From 1953 to 1959, he was with GEC, Stanmore, U.K., where he was involved with microwave components and systems. In 1959, he joined Mullard Research Laboratories, Redhill, U.K., where he developed a widely used technique for accurate instantaneous frequency measurement using several microwave discriminators in parallel known as digital IFM. This electronic countermeasures work included the development of decade bandwidth directional couplers and broad-band matching theory. From 1964 to 1967, he was a member of the faculty of The University of Leeds, Leeds, U.K., where he carried out research in microwave network synthesis, including distributed elliptic function filters and exact synthesis for branch-guide and multiaperture directional couplers. In 1967, he joined Microwave Development Laboratories, Natick, MA, as Vice President of Research. He developed practical techniques for the design of broad-band mixed lumped and distributed circuits, such as tapered corrugated waveguide harmonic rejection filters, and the synthesis of a variety of microwave passive components. This included the development of multioctave multiplexers in suspended substrate stripline, requiring accurate modeling of inhomogeneous stripline circuits and discontinuities. From 1984 to 1988, he was with KW Microwave, San Diego, CA, where he was mainly involved with design implementations and improvements in filter-based products. From August 1988 to July 1989, he was with Remec Inc., San Diego, CA, where he continued with advances in suspended substrate stripline components, synthesis of filters with arbitrary finite frequency poles, and microstrip filters. In July 1989, he became an independent consultant and has worked with many companies on a wide variety of projects, mainly in the field of passive components, especially filters and multiplexers. He has authored approximately 70 papers and two books, and holds 12 patents.

Dr. Levy has been involved in many IEEE Microwave Theory and Techniques Society (IEEE MTT-S) activities, including past editor of the IEEE TRANSACTIONS ON MICROWAVE THEORY AND TECHNIQUES (1986–1988). He was chairman of the Central New England and San Diego IEEE MTT-S Chapters, and was vice-chairman of the Steering Committee for the 1994 IEEE MTT-S International Microwave Symposium (IMS). He was the recipient of the 1997 IEEE MTT-S Career Award.

Peter Petre (S'90–M'92) received the M.S. and Ph.D. degrees in electrical engineering from the Technical University of Budapest, Budapest, Hungary, in 1985 and 1991, respectively.

He is currently a Senior Research Scientist in the Microwave Technology Department, Microelectronics Laboratory, HRL Laboratories, Malibu, CA. From 1990 to 1992, he was a Visiting Research Associate at Syracuse University, Syracuse, NY. From 1992 to 1996, he was the Electromagnetic Group Manager at Compact Software Inc. (now the Ansoft Corporation), where he was engaged in the development and management of Compact's commercially available three-dimensional full-wave electromagnetic simulator "Microwave Explorer." Since 1996, he has been with HRL Laboratories, where he has pioneered the microelectromechanical system (MEMS) tunable miniature filters and devices, as well as the fast numerical method in circuit simulation research. He also has extensive experience in the area of advanced microwave and millimeter-wave circuit and system development, such as filters, interconnects, MEMS devices, monolithic-microwave integrated-circuit (MMIC) antennas, and packaging. He has authored or co–authored over 50 journal and conference publications.